Supporting information

Nitrogen-doped graphene quantum dots-intensified tungsten oxide nanosheets as the SERS substrate for antibiotics detection

Lu Tan, ‡[bc] Xuanzhao Lu, ‡[c] Shuzhen Yue, [c] Yue Cao, [a] Yang Zhou, *[a] Baokang Jin, *[b] and Jun-Jie Zhu *[c]

[a] Key Laboratory for Organic Electronics & Information Displays and Institute of Advanced Materials, Nanjing University of Posts & Telecommunications (NJUPT), Nanjing 210023, PR China. E-mail: iamyangzhou@njupt.edu.cn

[b] Department of Chemistry, Anhui University, Hefei 230601, PR China. E-mail: bkjinhf@ aliyun.com

[c] State Key Laboratory of Analytical Chemistry for Life Science, School of Chemistry and Chemical Engineering, Nanjing University, Nanjing, Jiangsu 210023, PR China. E-mail: jjzhu@nju.edu.cn

‡ Lu Tan and Xuanzhao Lu contributed equally to this work.

Table of Contents

Experimental section

1. Materials and measurements

All of the chemical reagents used in this experiment were of analytical grade and used as received. Sodium tungstate dihydrate ($Na_2WO_4 \cdot 2H_2O$), citric acid, malachite green (MG), copper (II) phthalocyanine (CuPc) and benzyl butyl phthalatewere purchased from Aladdin-Reagent Co., Ltd. Urea, glucose, methylene blue (MB), and methyl orange (MO) were purchased from Sinopharm Chemical Reagent Co., Ltd. norfloxacin (NOR), ciprofloxacin (CIP) and doxycycline hydrochloride (DCH) were obtained from Shanghai Macklin Biochemical Co., Ltd. The ultrapure water was used as dispersant unless otherwise specified, which was obtained from a Milli-Q water purification system.

The X-ray diffraction (XRD) patterns for phase and crystal structure of the samples were obtained by Bruker Advanced D8 X-ray diffractometer (Cu Kα radiation source) from 10 ° to 80 ° (5 ° min^{-1}). The morphologies and microstructures of the samples were recorded on a Hitachi S4800 field-emission scanning electron microscopy (FESEM, 20 kV). Additionally, the detailed morphologies were characterized by Transmission electron microscopy (TEM) images on a JEM-1011 transmission electron microscope (100 kV). The X-ray photoelectron spectroscopy (XPS) was performed on a PHI5000 Versa Probe spectrometer (Al Kα as an X-ray source). The optical absorption spectra and band gap were examined on a UV-Vis-NIR spectrophotometer (Shimadzu, UV-3600) with 200 nm to 800 nm in the Ultraviolet-visible diffuse reflectance spectra (UV-vis DRS) mode, then transformed to the UV-Vis absorption spectra according to the Kubelka-Munk relationship. All the electrochemical measurements were measured on the CHI660E electrochemical workstation with the three-electrode quartz cell with 0.2 M of Na_2SO_4 aqueous solution (pH= 6.8) as the electrolyte. Before data collection, the scans were repeated for at least 10 times to reach a steady state. In addition, indium tinoxide (ITO) conducting glass coating with the different samples, platinum wire and Ag/AgCl (saturated KCl) electrode was applied as the working electrode, counter electrode and reference electrode, respectively. A Xenon lamp (150 W) was used as the light source in the photocurrent response measurement.

The Mott-Schottky plots were measured in the dark at a frequency of 1000 Hz.

2. The synthesis of WO_3 nanosheets (WO_3 NSs)

The WO_3 NSs were fabricated via a modified two-step method based on the previous literature.[1] Firstly, $WO_3 \cdot H_2O$ as the precursor was prepared. In a typical procedure, citric acid (1.5 mmol) and glucose (5 mmol) were sequentially added to 30 mL of $Na_2WO_4 \cdot 2H_2O$ (1 mmol) solution, under stirring until complete dissolution was achieved. Following this, 3 mL of hydrochloric acid (6 M) was carefully added dropwise to the reaction mixture, which was further stirred for an additional 30 minutes. The resulting reaction mixture was then transferred into a 50 mL stainless steel reactor, sealed, and subjected to heating at 120 °C for 24 hours. Upon natural cooling to room temperature, the resultant precipitate was collected via centrifugation and washed repeatedly with water and anhydrous ethanol to eliminate any residual impurities. Finally, the $WO_3 \cdot H_2O$ was dried overnight in an oven at 60 °C. Secondly, 1 g of the precursor was placed in a porcelain boat and further annealed for 120 min at 400 °C in the Muffle furnace with a heating rate of 2 °C·min^{-1}, the achieved powder was collected for further use and characterization.

3. The synthesis of N-doped graphene quantum dots (NGQDs)

The synthesis of NGQDs was carried out according to a previous literature with some modifications. [2] Briefly, Citric acid (0.2627 g) and urea (0.3 g) were mixed and dissolved in 6 ml of deionized water under the action of ultrasound. The solution was then transferred to a Teflon-lined stainless steel high-pressure reaction kettle, and heated at 160 ℃ for 8 hours. After allowing the reaction solution to cool naturally to room temperature, a certain amount of absolute ethanol was added, and the resulting precipitate was collected by centrifugation at 5000 rpm min^{-1} for 5 minutes.

4. The fabrication of NGQDs/WO_3 NSs

A hydrothermal method was employed to synthesise NGQDs/WO_3 NSs. In detail, a total of 50 mg of WO_3 nanosheets were dispersed in 30 mL of absolute ethanol, WO_3 nanosheets were dispersed in 30 mL of absolute ethanol for 30 minutes, followed by sonication of the solution for an additional 30 minutes. Subsequently, a certain amount of NGQDs solution was introduced to the aforementioned mixture. After sonication for

30 min, the mixture was transferred to a 50 mL Teflon-lined autoclave, and heated at 140 °C for 3 h. The reaction product was then subjected to centrifugation and washed twice with water and ethanol. For further applications, the final NGQDs/WO_3 NSs composite was vacuum dried and stored.

5. Raman measurement

The Raman enhancement activity of the substrate materials was evaluated using MB, MG, MO and CuPc. Typically, a sample (10 mg) was dispersed in deionized water (10 mL) and treated with ultrasonication to obtain a uniform dispersion. Then, 20 μL of the dispersion was dropped onto a glass slide (0.25 cm^2) and dried in a vacuum oven at 60 °C to form a homogeneous sample film. Subsequently, 10 μL of a Raman molecular solution was applied to the prepared substrate and dried at 60 °C for 30 minutes. Finally, Raman testing was conducted. A reflectance confocal microscopy Raman spectroscopy system (inVia, Renishaw, UK) was used with a 633 nm laser as the excitation source. The laser power was set to 1.7 mW, and a 20 × objective lens was selected to collect the Raman spectra. The sampling time was set to 10 seconds, and the intensities of five random points were collected and averaged for data analysis.

6. Detection in practical samples

The detection of antibiotics in real water samples was verified using the prepared SERS substrates. Wastewater samples were collected from the Nanjing xianlin wastewater treatment Plant. Both the wastewater and tap water samples were filtered using a 0.22 μm filter before being used as dispersants to prepare antibiotic solutions of specific concentrations for Raman testing.

7. Calculation of the energy levels

The energy levels were calculated based on the data obtained from ultraviolet-visible diffuse reflectance spectroscopy and Mott-Schottky tests, along with the relevant potential conversion equations. [3] In detail, the flat-band potential (E_{fb}) is determined by reading the x-axis intercept of the Mott-Schottky plot. The conductive band (E_{CB}) level is 0.1 V lower than the E_{fb}, allowing for the derivation of the valence band energy level. The obtained E_{fb} (*vs. Ag/AgCl*) should be transferred to the normal hydrogen electrode (NHE) by a relationship as:

$$E_{NHE} = E_{Ag/AgCl} + 0.197$$

The band gap (E_g) is calculated by the Tauc plot.

$$\alpha hv = A\left(hv - E_g\right)^n$$

where *α, h, v, A* and E_g are the absorption coefficient, Planck's constant, light frequency, proportionality constant and band gap, respectively.

The valence band (E_{VB}) is obtain by the equation as:

$$E_{VB} = E_{CB} - E_g$$

where E_{CB} labels the energy level of CB, E_{VB} is the energy level of VB and E_g is the band gap.

The corresponding energy levels for the vacuum could be calculated by subtracting the energy level from the − 4.5 eV

8. Calculations of enhancement factor (EF)

The enhancement factor (EF) is calculated to estimate the potentiation of the proposed substrate according to the following equations [4]:

$$EF = \frac{I_{SERS}}{I_{bulk}} \times \frac{N_{bulk}}{N_{SERS}}$$

where I_{SERS} and I_{bulk} represent the peak intensities of SERS and the normal Raman at 1623 cm^{-1}. Simultaneously, N_{SERS} and N_{bulk} ars the valid molecule number on the substrate and the practical number of probe molecules in the Raman detection view.

The number of probe molecules (N_{bulk}) in standard Raman detection can be calculated in the following equation:

$$N_{bulk} = \frac{\rho h S_{Raman} N_A}{M}$$

where S_{Raman} is the laser radiation area, *M* is the molecular weight (319.85 g mol^{-1}) and N_A is the Avogadro constant.

$$S_{Raman} = \pi(\frac{d_{laser}}{2})^2$$

d_{laser} is the diameter of the laser, and it could be inferred from the following equation:

$$d_{laser} = \frac{1.22\lambda}{N.A.}$$

λ is the wavelength of the laser (633 nm) and *N.A.* represents the numerical

aperture of 20× objective (*N.A.* = 0.4).

$$h = \frac{3.28\eta d_{laser}}{N.A.}$$

η is the refractive index of water (1.33). ρ is the density of bulk MB (1.0448 g cm^{-3}) and h is the laser radiation depth, which could be calculated to be 21 μm.

Given that the molecules were distributed in a monolayer on the substrate, and the valid probe number on substrate in the SERS detection can be calculated using the following equation:

$$N_{SERS} = CVN_A \frac{S_{SERS}}{S_{substrate}}$$

Where, C is the molar concentration of the analyte solution, V is the volume of the droplet, N_A is the Avogadro constant, S_{SERS} is the area of laser radiation in SERS detection, similar to S_{Raman} in the same conditions. $S_{substrate}$ is the area of the substrate (0.25 cm^2).

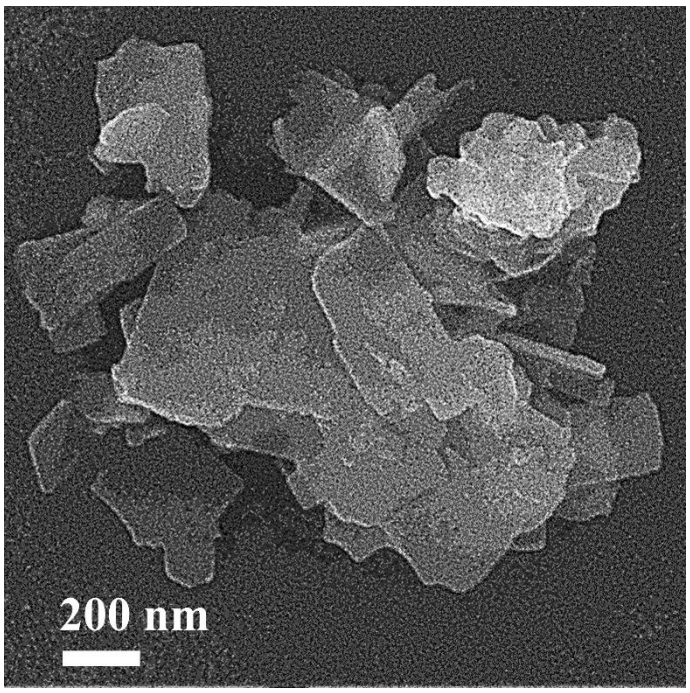

Fig. S1 The SEM image of WO_3 NSs.

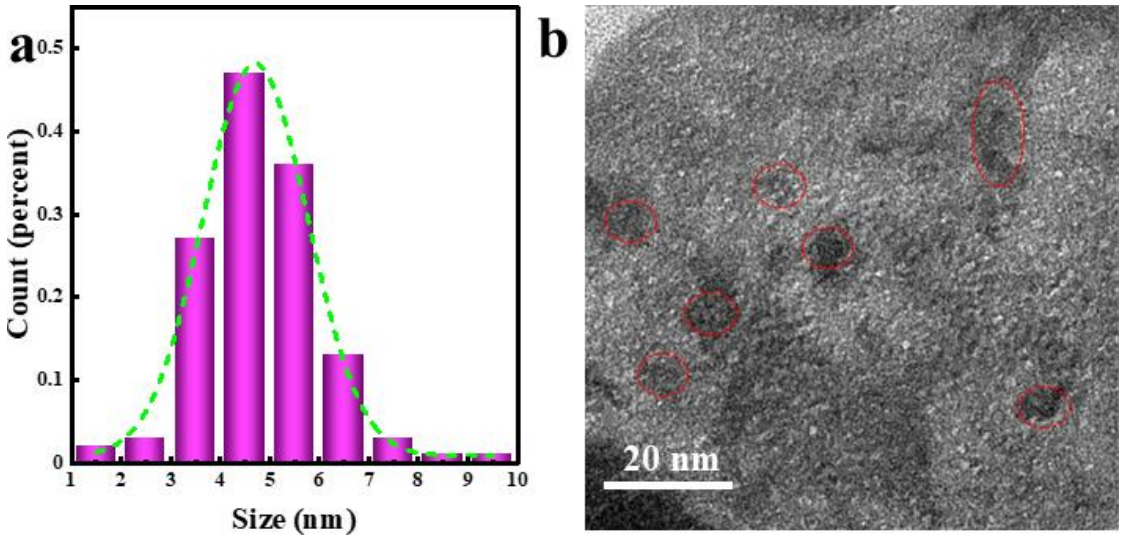

Fig. S2 (a) The size distribution of NGQDs and (b) the TEM image of NGQDs/WO_3 NSs.

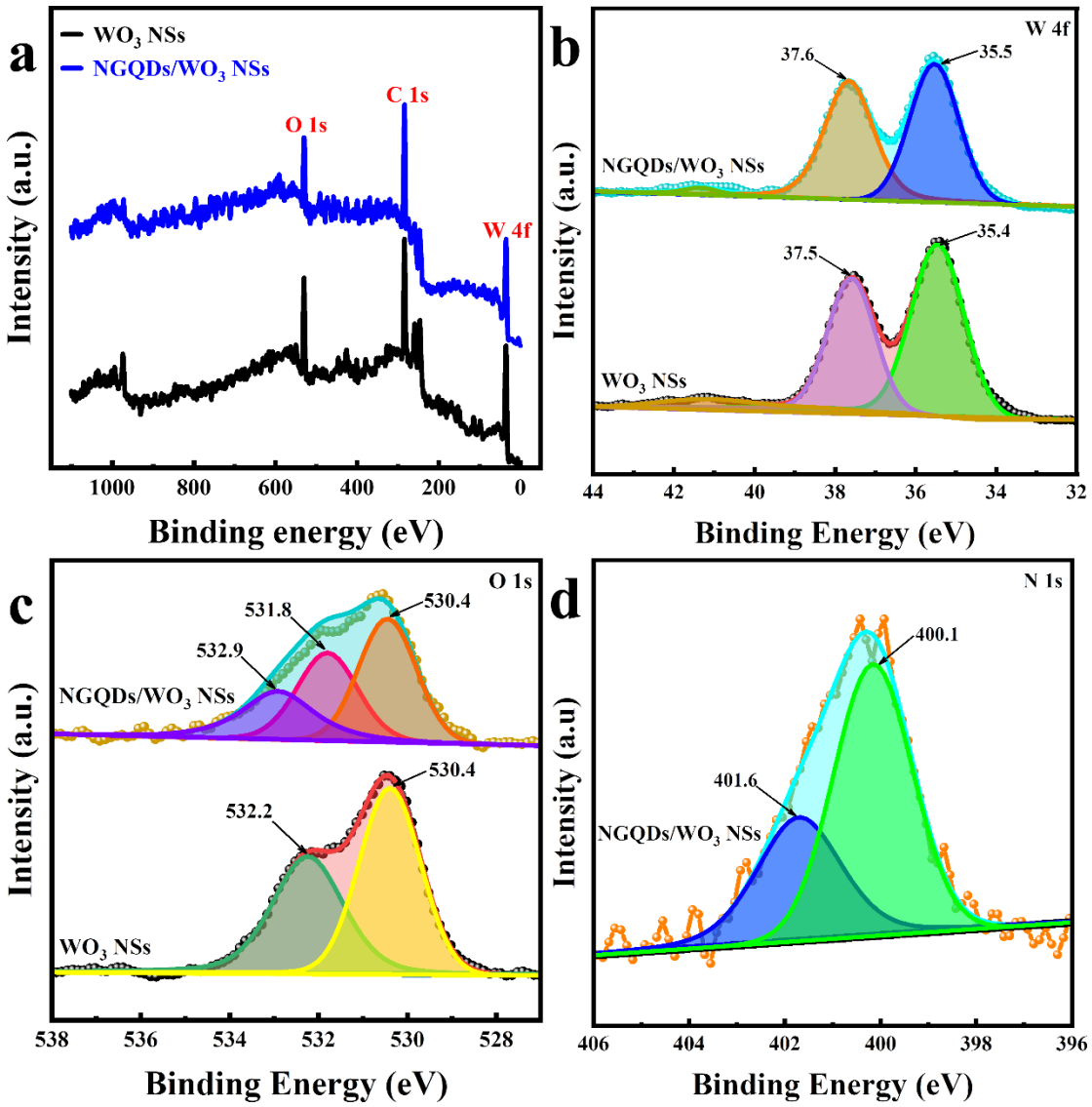

Fig. S3 (a) the XPS survey spectra, (b) W 4f, (c) O 1s and (d) N 1s XPS spectrum of WO_3 NSs and NGQDs/WO_3 NSs.

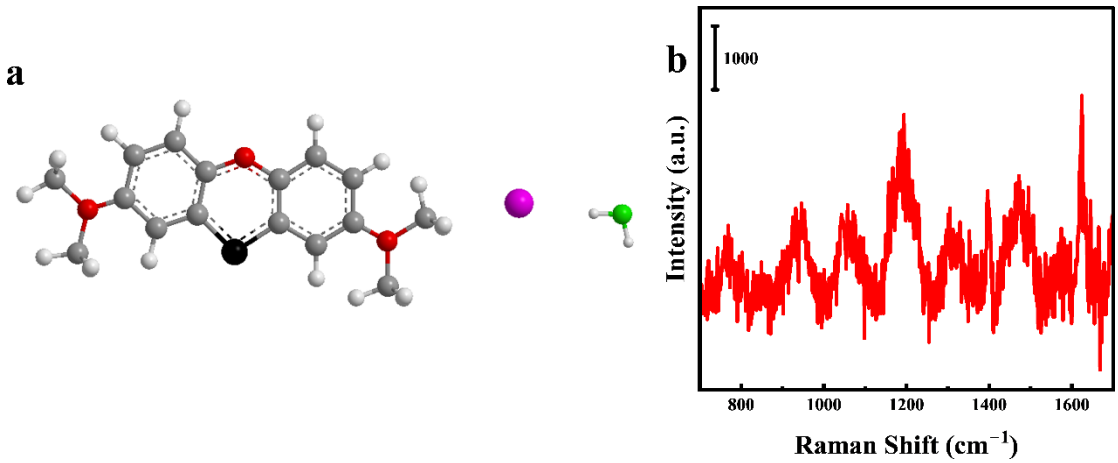

Fig. S4 (a) The chemical formula and (b) Raman spectrum of MB.

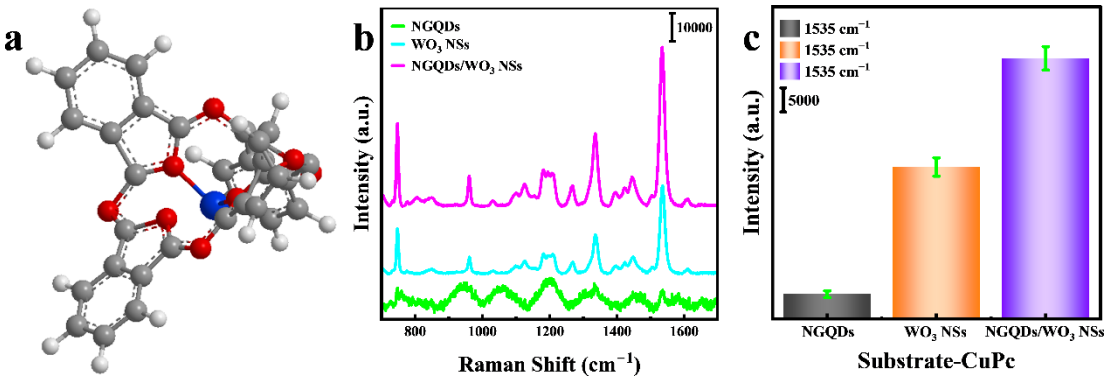

Fig. S5 (a) The chemical formula, (b) Raman spectra and (c) the corresponding intensity at 1535 cm^{-1} of fingerprint peak for CuPc (10^{-5} M) on the NGQDs, WO_3 NSs and NGQDs/WO_3 NSs.

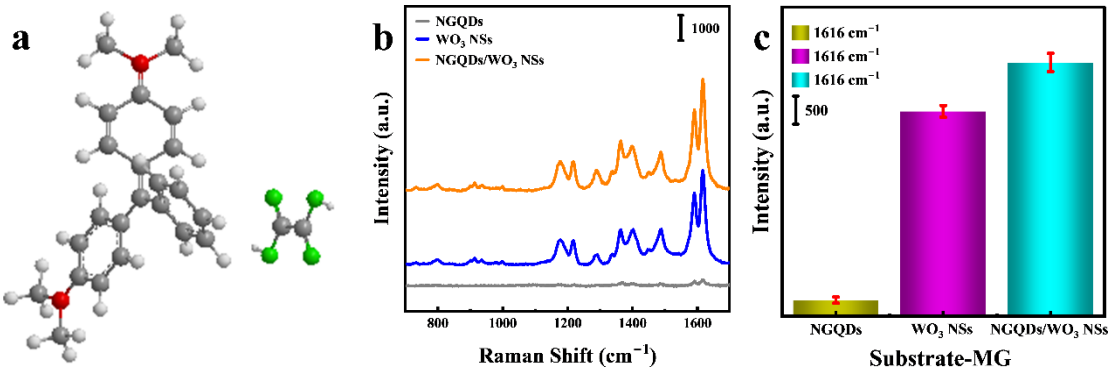

Fig. S6 (a) The chemical formula, (b) Raman spectra and (c) the corresponding intensity at 1616 cm^{-1} of fingerprint peak for MG (10^{-5} M) on the NGQDs, WO_3 NSs and NGQDs/WO_3 NSs.

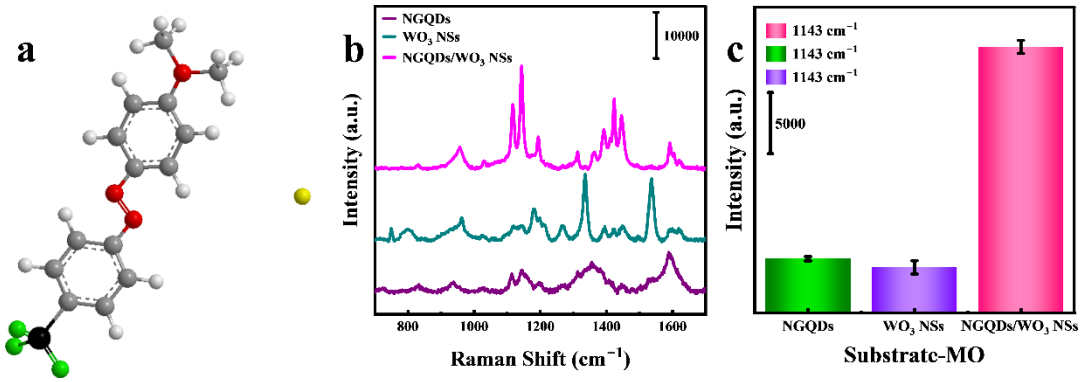

Fig. S7 (a) The chemical formula, (b) Raman spectra and (c) the corresponding intensity at 1143 cm^{-1} of fingerprint peak for MO (10^{-5} M) on the NGQDs, WO_3 NSs and NGQDs/WO_3 NSs.

Furthermore, three additional Raman probe molecules (malachite green (MG), copper (II) phthalocyanine (CuPc) and methyl orange (MO)), each with distinct characteristic peaks, were selected to measure the potentiation of NGQDs/WO_3 NSs substrate (Fig. S5 – S7). The results not only confirmed the substrate's SERS universality but also highlighted the exceptional SERS properties.

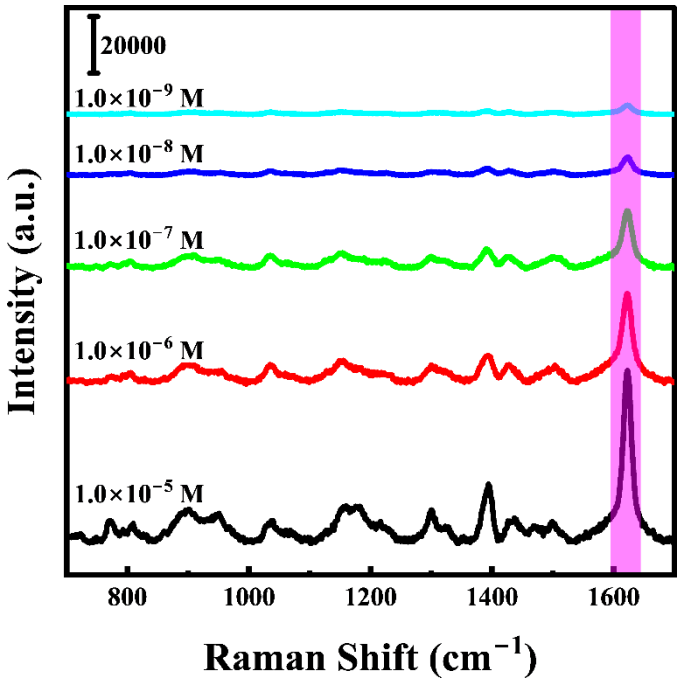

Fig. S8 The SERS spectra of MB at various concentrations (10^{-5} M to 10^{-9} M) collected on the NGQDs/WO_3 NSs substrate.

As shown in Fig. S8, the Raman peak intensity gradually decreased with the decrease in the range of 10^{-5} to 10^{-9} M.

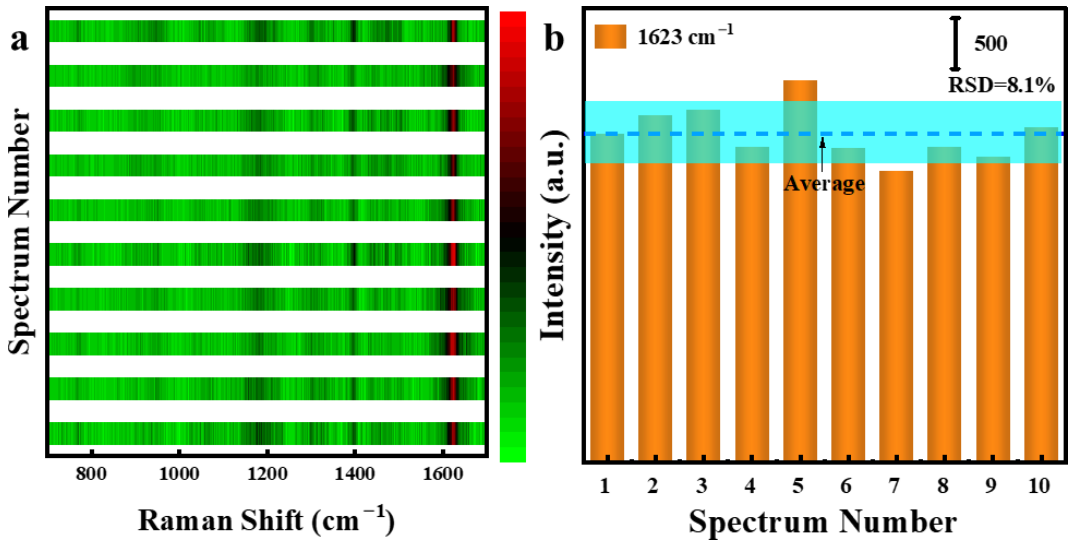

Fig. S9 (a) SERS spectra heatmap of the random 10 spots for MB (10^{-5} M) collected on the NGQDs/WO_3 NSs substrate and (b) the corresponding intensity at 1623 cm^{-1}.

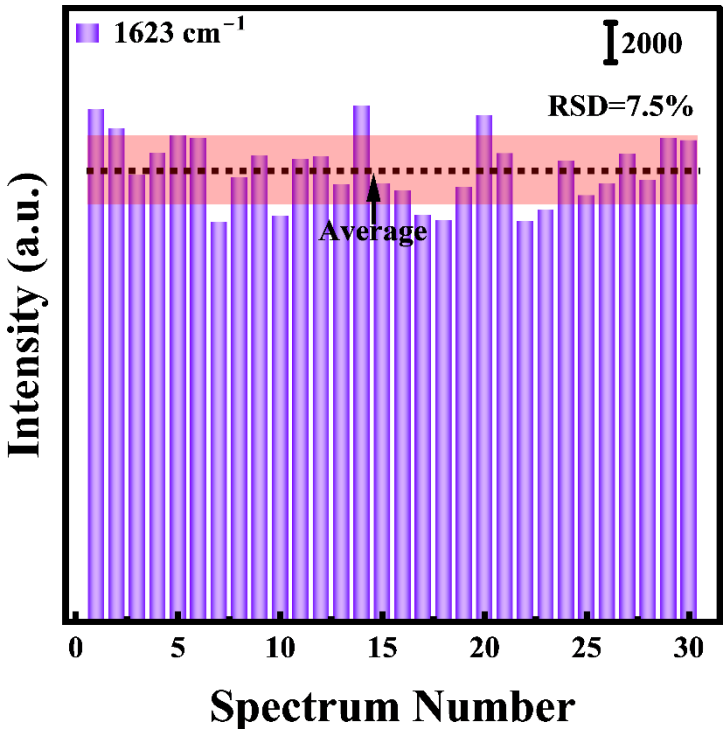

Fig. S10 The corresponding intensity at 1623 cm^{-1} in Fig. 2e.

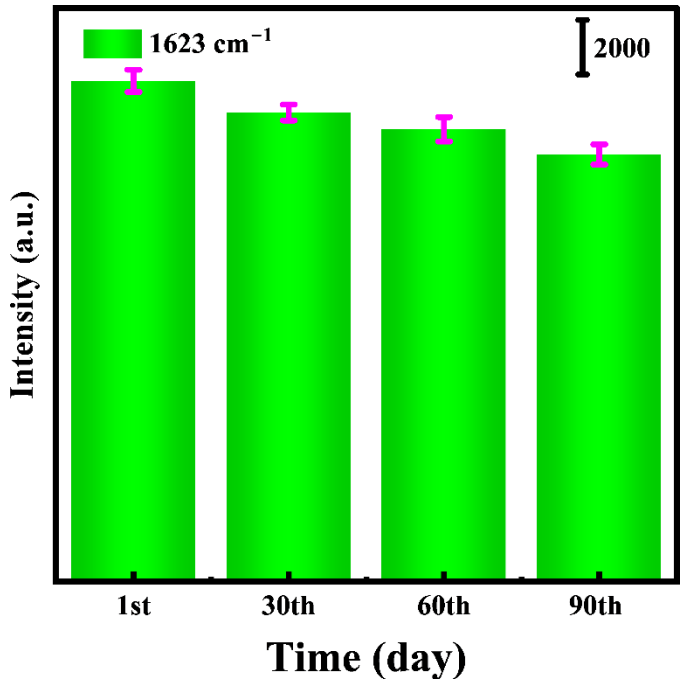

Fig. S11 The corresponding intensity at 1623 cm^{-1} in Fig. 2f.

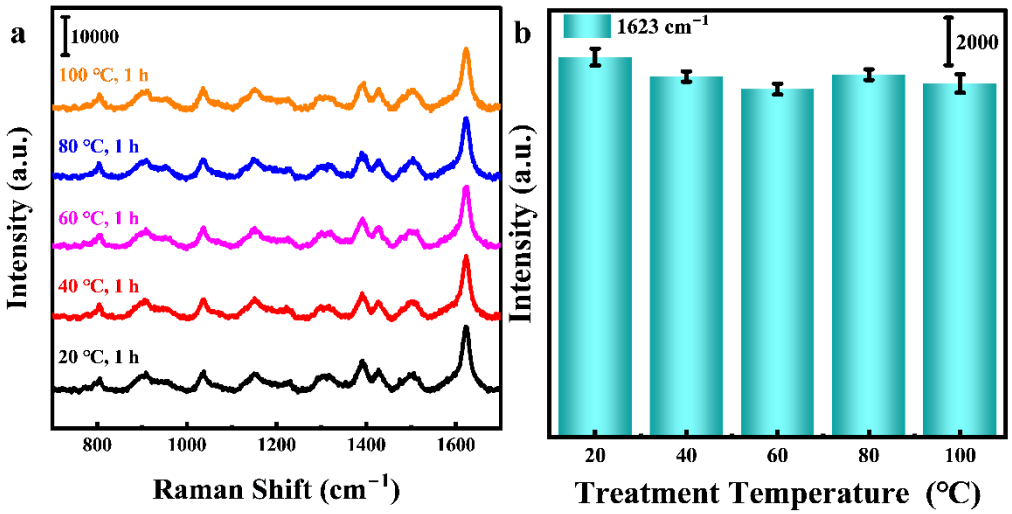

Fig. S12 The thermal stability test of NGQDs/WO_3 NSs substrate during the treatment at different temperature for 1 h. (a) the Raman spectra of MB (10^{-5} M) on NGQDs/WO_3 NSs treated at different temperature for 1 h and (b) the corresponding intensity at 1623 cm^{-1}.

As shown in Fig. S12, the Raman activity of the substrates did not change significantly even after treatment at temperatures up to 100 °C, highlighting the excellent thermal stability of the prepared NGQDs/WO_3 NSs substrates.

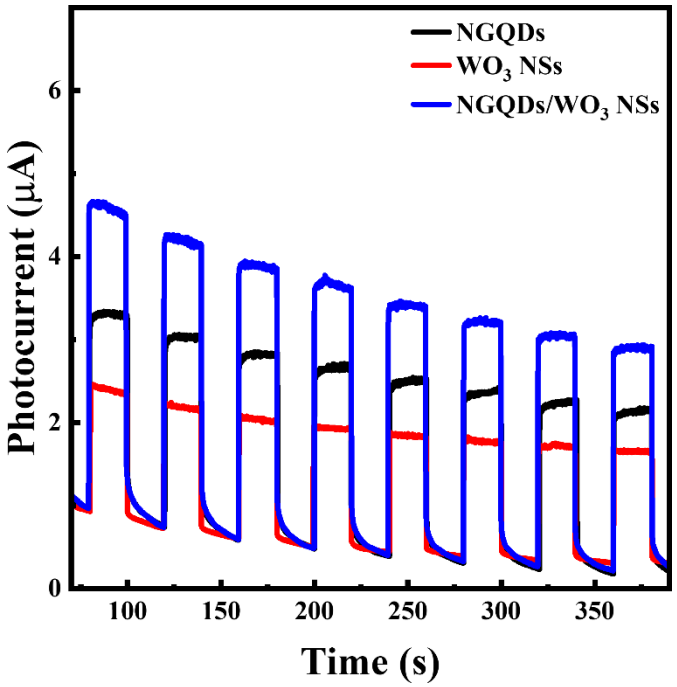

Fig. S13 Transient photocurrent responses of NGQDs, WO_3 NSs and NGQDs/WO_3 NSs in 0.2 M Na_2SO_4 aqueous solutions (pH= 6.8) under the irradiation of visible light with light on and off every 20 seconds.

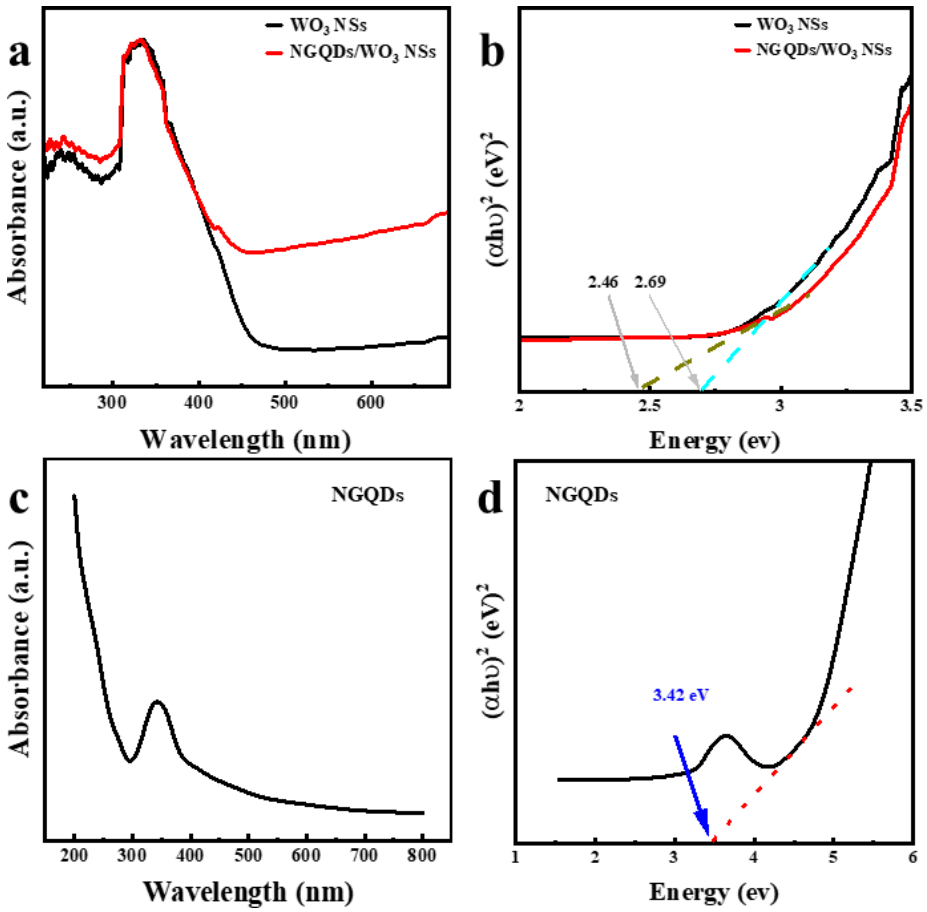

Fig. S14 (a, c) UV–vis DRS spectra and (b, d) the band gap of the samples.

The band gap energies (E_g) of WO_3 NSs and NGQDs/WO_3 NSs were calculated using UV-vis diffuse reflectance spectroscopy (DRS) and Tauc plot.

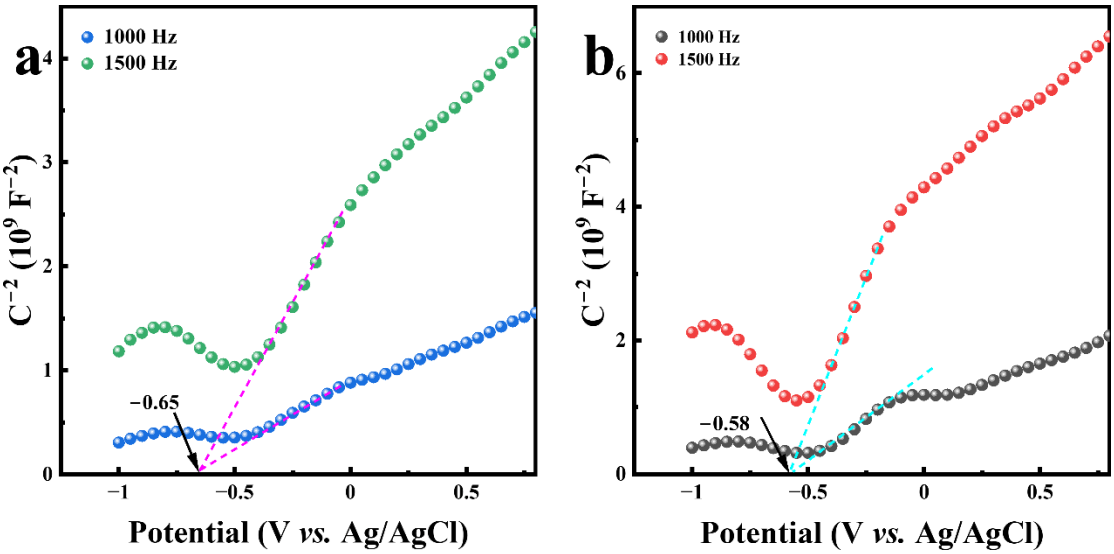

Fig. S15 Mott-Schottky plots of the (a) WO_3 NSs and (b) NGQDs/WO_3 NSs.

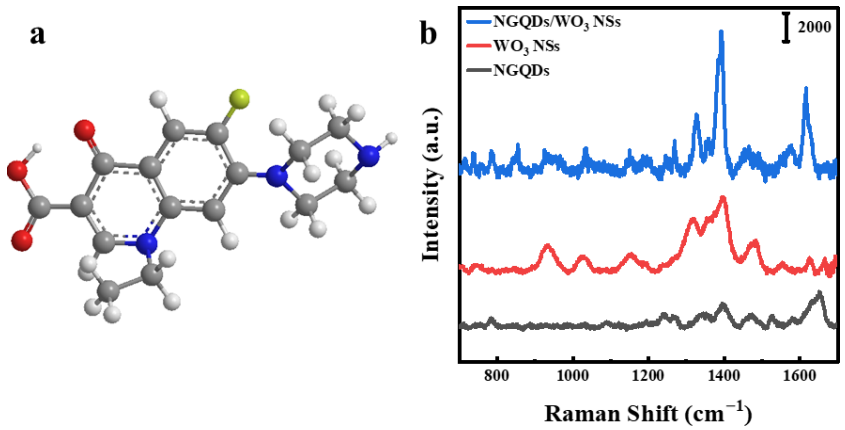

Fig. S16 The chemical formula of NOR and the SERS spectra of NOR (10^{-4} M) on NGQDs, WO_3 NSs and NGQDs/WO_3 NSs.

Norfloxacin (NOR), a fluoroquinolone antibiotic, is extensively used to treat urinary, respiratory, and gastrointestinal infections. However, residues resulting from overuse or misuse can lead to neurological disorders, antibiotic resistance, and hinder bone development in children.

As shown in Fig. S16b, A higher SERS intensity of NOR can be detected on NGQDs/WO_3 NSs compared to NGQDs and WO_3 NSs, demonstrating the superiority of NGQDs/WO_3 NSs and its feasibility for antibiotic detection.

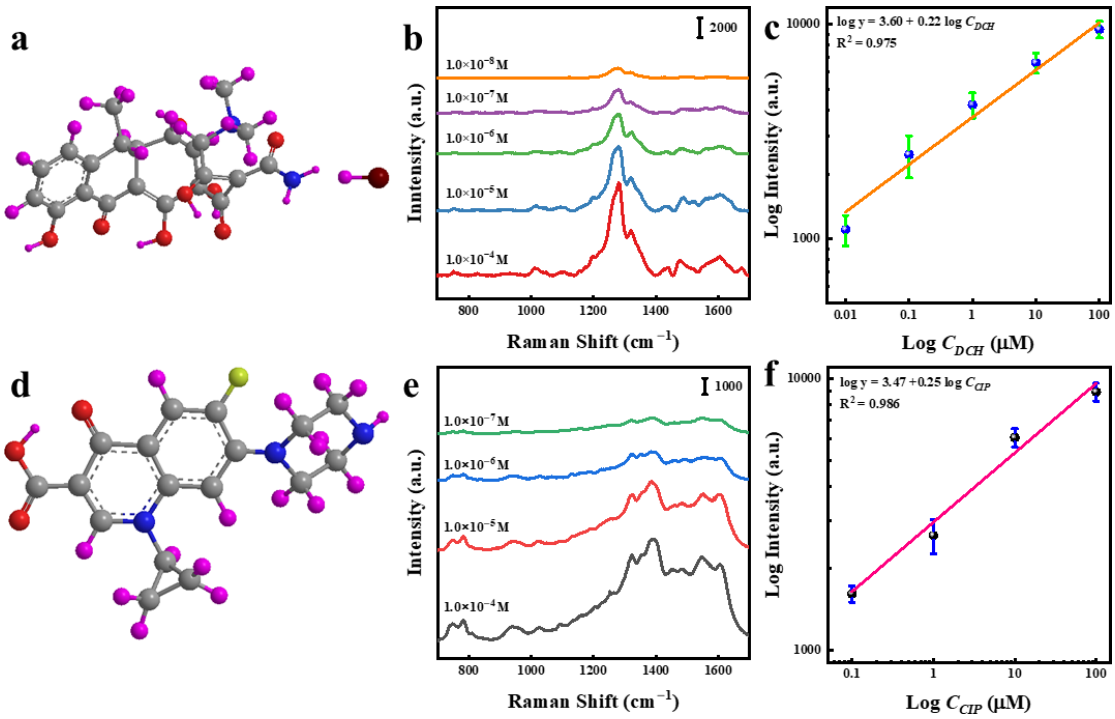

Fig. S17 (a) The chemical formula, (b) the SERS spectra at various concentrations (10^{-4} M to 10^{-8} M) collected on the NGQDs/WO_3 NSs substrate in wastewater and (c) the fitted linear plot of the logarithmic intensities at 1282 cm^{-1} with logarithmic concentrations of DCH. (d) The chemical formula, (e) The SERS spectra of CIP at various concentrations (10^{-4} M to 10^{-7} M) collected on the NGQDs/WO_3 NSs substrate in wastewater and (f) the fitted linear plot of the logarithmic intensities at 1393 cm^{-1} with logarithmic concentrations of CIP.

Table S1 Raman shifts (cm^{-1}) and assignments for MB.[5]

Normal Raman (cm^{-1})	SERS (cm^{-1})	Assignments
768	772	In-plane bending of C-H
945	950	In-plane bending of C-H
1057	1060	In-plane bending of C-H
1182	1189	Stretching of C-N
1304	1300	Stretching of C-N
1396	1394	Symmetrical stretching of C-N
1474	1468	Asymmetrical stretching of C-N
1624	1623	Ring stretching of C-C

Table S2 Comparisons of the LOD for MB with previous methods.

Target	Method	Linear range (M)	LOD (M)	Ref.
MB	Electrochemistry	1.0×10^{-8}-5.0×10^{-5}	2.1×10^{-10}	6
	Electrochemistry	1.0×10^{-7}-1.0×10^{-3}	4.7×10^{-9}	7
	SERS	1.0×10^{-7}-1.0×10^{-3}	1.0×10^{-7}	8
	SERS	1.0×10^{-9}-5.0×10^{-5}	1.3×10^{-10}	This work

Table S3 Comparisons of the LOD and EF for MB with other SERS substrates.

No.	substrate	LOD (M)	EF	Ref.
1	Graphene/Ge	1.0×10^{-7}	---	9
2	MoO_2/GO	1.0×10^{-9}	1.0×10^{7}	10
3	fluorinated graphene	1.0×10^{-7}	1.6×10^{3}	8
4	Ag_2S NWs	1.0×10^{-7}	4.0×10^{4}	11
5	NGQDs/WO_3 NSs	1.3×10^{-10}	2.3×10^{5}	This work

Table S4 Recovery of NOR, DCH and CIP in wastewater via SERS method with the proposed substrate.

Antibiotic	Spiked (M)	Determined (M)	Recovery (%)	RSD (%)
NOR	1.0×10^{-4}	0.974×10^{-4}	97.4	2.68
	1.0×10^{-5}	1.011×10^{-5}	101.1	2.33
	1.0×10^{-6}	0.966×10^{-6}	96.6	3.25
	1.0×10^{-7}	0.928×10^{-7}	92.8	4.86
	1.0×10^{-8}	0.895×10^{-8}	89.5	6.08
DCH	1.0×10^{-4}	0.963×10^{-4}	96.3	2.84
	1.0×10^{-5}	0.975×10^{-5}	97.5	2.91
	1.0×10^{-6}	1.014×10^{-6}	101.4	3.68
	1.0×10^{-7}	0.932×10^{-7}	93.2	4.99
	1.0×10^{-8}	0.908×10^{-8}	90.8	6.24
CIP	1.0×10^{-4}	0.954×10^{-4}	95.4	4.28
	1.0×10^{-5}	0.967×10^{-5}	96.7	3.94
	1.0×10^{-6}	0.904×10^{-6}	90.4	5.26
	1.0×10^{-7}	0.899×10^{-7}	89.9	5.69

References

1. Z. Zhou, X. Wang, H. Zhang, H. Huang, L. Sun, L. Ma, Y. Du, C. Pei, Q. Zhang, H. Li, L. Ma, L. Gu, Z. Liu, L. Cheng and C. Tan, *Small*, 2021, **17**, 2007486.
2. H. Kishida and M. H. Mikkelsen, *Nano Lett.*, 2022, **22**, 904-910.
3. H. Li, M. Chuai, X. Xiao, Y. Jia, B. Chen, C. Li, Z. Piao, Z. Lao, M. Zhang, R. Gao, B. Zhang, Z. Han, J. Yang and G. Zhou, *J. Am. Chem. Soc.*, 2023, **145**, 22516-22526.
4. S. Chen, S. Weng, Y.-H. Xiao, P. Li, M. Qin, G. Zhou, R. Dong, L. Yang, D.-Y. Wu and Z.-Q. Tian, *J. Am. Chem. Soc.*, 2022, **144**, 13174-13183.
5. M. Liu, W. Liu, W. Zhang, P. Duan, M. Shafi, C. Zhang, X. Hu, G. Wang and W. Zhang, *ACS Appl. Mater. Interfaces*, 2022, **14**, 56975-56985.
6. M. Hayat, A. Shah, J. Nisar, I. Shah, A. Haleem and M. N. Ashiq, *Catalysts*, 2022, **12**, 306.
7. T.-C. Lin, Y.-S. Li, W.-H. Chiang and Z. Pei, *Biosens. Bioelectron.*, 2017, **89**, 511-517.
8. L. Que, J. Ai, T. Shao, R. Han, J. Su, Y. Guo, Y. Liu, J. Li, X. Jian and Z. Zhou, *Appl. Surf. Sci.*, 2023, **616**, 156496.
9. Z. He, L. Yu, G. Wang, C. Ye, X. Feng, L. Zheng, S. Yang, G. Zhang, G. Wei, Z. Liu, Z. Xue and G. Ding, *ACS Appl. Mater. Interfaces*, 2022, DOI: 10.1021/acsami.2c00584.
10. J. Chen, K. Sun, Y. Zhang, D. Wu, Z. Jin, F. Xie, X. Zhao and X. Wang, *Anal. Bioanal. Chem.*, 2019, **411**, 2781-2791.
11. Y.-C. Chen, Y.-M. Bai and Y.-K. Hsu, *J. Alloys Compd.*, 2021, **881**, 160647.